# On the Accuracy of Upwinding Schemes for Hyperbolic Systems with Source Terms

Jean-Marc Hérard, Olivier Hurisse

# On the Accuracy of Upwinding Schemes for Hyperbolic Systems with Source Terms

Jean-Marc Hérard *
*EDF-DRD, 78401 Chatou cedex, France*
Olivier Hurisse†
*Université Aix-Marseille I, 13453 Marseille cedex 13, France*

**The paper is devoted to the computation of a simple model which describes the motion of two-phase flows including source terms. The strategy of upwinding of source terms is investigated and compared with the standard fractional step method. A first one relies on the usual fractional step approach. The second and third ones apply for the notion of upwinding of source terms. A detailed numerical study which includes some measure of the $L^1$ norm of the error enables a true comparison of the latter schemes.**

## I. Introduction

Almost all two-phase flow models contain contributions connected with convective effects and with so-called source terms. The latter aim at describing interface phenomena. These should at least describe mass transfer and interfacial momentum transfer. They may be seen as relaxation terms to some mechanical equilibrium ($U_1 = U_2$), or thermodynamical equilibrium. Time to relaxation essentially depends whether one accounts for condensation, flashing or evaporation effects. As a consequence, stiffness of source terms is variable, and may be dominant over convective effects, or on the contrary be completely negligible. Another important issue is whether the flow is steady or not. Depending on all these situations, one has to cope with both (non)homogeneous convective systems which may turn locally (in space or time) to ordinary differential equations.

In order to compute these systems, we may roughly say that two distinct strategies have been developed up to now: (i) the first one is refered to as the fractional step approach : it simply consists in two steps. In the first one, pure advection is achieved, whereas in the second one, (stiff) source terms are approximated. The main advantages are the following. The resulting scheme is much stable ; one may apply for "standard" hyperbolic schemes to discretize first order terms ; eventually, this decouples effects so that users who are not familiar with upwinding techniques may concentrate on the sources; (ii) in the second one, which has been introduced some time ago by LeRoux and co-authors in order to compute *steady* nonhomogeneous hyperbolic systems, source terms are "upwinded", in order to represent perfectly steady states on coarse meshes (see[1–5]) This has been motivated by the rather poor behaviour (more precisely the poor accuracy) of the fractional step approach (noted FS afterwards) in these steady situations. We nonetheless recall that there is no loss of stability of the FS method, since one may check that the FS method still provides convergent approximations when the mesh is refined. Since we wish to have a better understanding of what strategy

*Research Engineer, Département MFTT, 6 quai Watier, and Associate Research Director, CNRS, LATP, AIAA Member
†PhD student, CMI-LATP, 39 rue Joliot Curie

should be retained in order to couple mixed systems through interfaces, considering *either steady or unsteady flows*, we at least need to investigate the true behaviour of *unsteady* solutions when sources are active. This is the main purpose of the present work.

In order to get a sufficiently accurate idea of the global behaviour of these schemes, we have chosen a three-equation model, which models the isentropic flow of a mixture of two species, which may exchange mass. Hence the physical unknowns are the total density, the mass fraction, and the mean velocity of the mixture. We assume that the pressure field only depends on the total density, which simplifies much the structure of solutions of equations, but should not be considered as a physically relevant closure. We afterwards will introduce the two cell candidates, and detail the interface solvers. All rely on the approximate Godunov approach (see[6–8]) but we insist that conclusions would be identical if one uses an exact Godunov scheme instead (see[9, 10]). Measure of the $L^1$ norm of the error in *unsteady* test cases enables to get a precise idea of true advantages and drawbacks of cell and interface schemes. It will clearly appear that none among the two strategies may be disregarded, since: (i) the FS method behaves rather well in all *unsteady* situations on coarse meshes; (ii) the upwind approach should be prefered when *steady* approximations are searched. This work is a contribution to the NEPTUNE joint project launched by EDF and CEA (see[11]). It is linked with recent investigations,[12–16] which aim at improving the interfacial coupling of two-phase models.

## II. A simplified model to describe reacting flows

We will start with a simple model which describes the motion of a mixture including two species with reacting terms. The convective part of the model is in conservative form, and we define the conservative variable $W = {}^t(\rho, \rho\alpha, \rho u)$, where $\rho$ stands for the mean density of the mixture, $u$ is the mean velocity in the field, and $\alpha$ is the concentration of some reacting component which is expected to lie in $[0, 1]$:

$$\frac{\partial \rho}{\partial t} + \frac{\partial \rho u}{\partial x} = 0 \tag{1}$$

$$\frac{\partial \rho\alpha}{\partial t} + \frac{\partial \rho\alpha u}{\partial x} = \rho s(\alpha) \tag{2}$$

$$\frac{\partial \rho u}{\partial t} + \frac{\partial \rho u^2 + P(\rho)}{\partial x} = \frac{\partial \mu \dfrac{\partial u}{\partial x}}{\partial x} \tag{3}$$

The source term $s$ depends on $\alpha$ and involve some constant time scale $\tau_0$, $\mu$ is a positive constant, and the function $P(\rho)$ is increasing, and such that $P(0) = 0$. The flux is $F(W) = (\rho u, \rho\alpha u, \rho u^2 + P(\rho))$. From time to time we will precise some specific form for the source term $s(\alpha)$, that is:

$$s(\alpha) = \frac{\alpha_{eq} - \alpha}{\tau_0}$$

with $\alpha_{eq}$ in $I_{adm} = [0, 1]$. Hence, we get (see[17] for proof).

Property 1
*An entropy pair* $(\eta(W), F_\eta(W))$ *for the system* (1)-(3) *is* $(\eta(W), F_\eta(W))$ *with:*

$$\eta(W) = \tfrac{\rho u^2}{2} + \rho\psi_1(\rho) + \rho\psi_2(\alpha)$$
$$F_\eta(W) = (\eta(W) + P(\rho))u$$

*with* $\psi_1(\rho) = \int_0^\rho (\frac{P(a)}{a^2} da)$ *and* $\psi_2(\alpha) = -\int_0^\alpha s(a)da$. *The entropy* $\eta(W)$ *is strictly convex with respect to*

*$W$, if and only if $s'(\alpha) < 0$, and the following entropy inequality holds for regular solutions of* (1)-(3)*:*

$$\frac{\partial \eta(W)}{\partial t} + \frac{\partial F_\eta(W)}{\partial x} - \frac{\partial \mu u \frac{\partial u}{\partial x}}{\partial x} < -\rho s^2 \tag{4}$$

One may check that the homogeneous convective set (or left hand side) of system (1)-(3):

$$\frac{\partial \rho}{\partial t} + \frac{\partial \rho u}{\partial x} = 0 \tag{5}$$

$$\frac{\partial \rho \alpha}{\partial t} + \frac{\partial \rho \alpha u}{\partial x} = 0 \tag{6}$$

$$\frac{\partial \rho u}{\partial t} + \frac{\partial \rho u^2 + P(\rho)}{\partial x} = 0 \tag{7}$$

is hyperbolic, since eigenvalues are real and distinct unless vacuum arises: $\lambda_1 = u - c$, $\lambda_2 = u$, $\lambda_3 = u + c$. Fields 1 and 3 are genuinely non linear, and the 2 field is linearly degenerated. The entropy inequality ensures that the jump of $U$ is negative through shock waves: $u_r - u_l < 0$, if subscripts $l, r$ respectively denote the states on the left and right side of the traveling shock wave. The construction of the entropy-consistent solution (composed of constant states separated by shock waves , rarefaction waves and contact discontinuities) of the one dimensional Riemann problem associated with the set ((5),(7)) with no vacuum occurrence (i.e. $\rho > 0$) is classical, and thus is not recalled herein. Existence and uniqueness of the solution is ensured if and only if the initial data agrees with:

$$u_R - u_L < \int_0^{\rho_L} \frac{c(a)}{a} da + \int_0^{\rho_R} \frac{c(a)}{a} da$$

In addition, the solution of the 1D Riemann problem is such that the maximum principle for the void fraction $\alpha$ holds. We only briefly recall the structure of the solution. The 1-wave and the 3 wave admit the following Riemann invariants: $I^1 = \{u + g(\rho), \alpha\}$, and $I^3 = \{u - g(\rho), \alpha\}$ respectively, where: $g(\rho) = \int_0^\rho \frac{c(a)}{a} da$. Besides, the Riemann invariants in the 2-wave are $I^2 = \{u, P\}$. An important point to note is that $\alpha$ may not vary in a 1-shock or in a 3-shock. As a consequence, the maximum principle for $\alpha$ is easily obtained.

We now introduce some function $A(x,t)$ such that $A(x, t = 0) = x$. Equations may be rewriten:

$$\frac{\partial A}{\partial t} = 0 \tag{8}$$

$$\frac{\partial \rho}{\partial t} + \frac{\partial \rho u}{\partial x} = 0 \tag{9}$$

$$\frac{\partial \rho \alpha}{\partial t} + \frac{\partial \rho \alpha u}{\partial x} - \rho s \frac{\partial A}{\partial x} = 0 \tag{10}$$

$$\frac{\partial \rho u}{\partial t} + \frac{\partial \rho u^2 + P(\rho)}{\partial x} = 0 \tag{11}$$

The non conservative system (8)-(11) is hyperbolic, since eigenvalues are real and distinct:$\lambda_1 = 0$, $\lambda_2 = u$, $\lambda_3 = u - c$ , $\lambda_4 = u + c$, unless vacuum arises, or if $u = 0$. Fields 3 and 4 are genuinely non linear, and the 1 and 2 fields are linearly degenerated. For conveniency, we will use $Z = (A, \alpha, \rho, u)$. Regular solutions of

previous system are governed by:

$$\frac{\partial A}{\partial t} = 0 \tag{12}$$

$$\frac{\partial \alpha}{\partial t} + u\frac{\partial \alpha}{\partial x} - s(\alpha)\frac{\partial A}{\partial x} = 0 \tag{13}$$

$$\frac{\partial \rho}{\partial t} + u\frac{\partial \rho}{\partial x} + \rho\frac{\partial u}{\partial x} = 0 \tag{14}$$

$$\frac{\partial u}{\partial t} + u\frac{\partial u}{\partial x} + \frac{P'(\rho)}{\rho}\frac{\partial \rho}{\partial x} = 0 \tag{15}$$

or in a condensed form: $\frac{\partial Z}{\partial t} + C(Z)\frac{\partial Z}{\partial x} = 0$. The field 1 and field 2 are linearly degenerated and the Riemann invariants associated with the 1-wave and the 2-wave are: $J^1 = \{u, \rho, A + u\phi(\alpha)\}$ , $J^2 = \{u, \rho, A\}$, where $\phi$ is defined for $s(\alpha) \neq 0$ as:

$$\phi'(\alpha) = -\frac{1}{s(\alpha)}$$

The field 3 and field 4 are genuinely non linear and the Riemann invariants associated with the 3-wave and the 4-wave are: $J^3 = \{u + g(\rho), \alpha, A\}$, $J^4 = \{u - g(\rho), \alpha, A\}$. In the limit case where $u = 0$, both sets $J^1$ and $J^2$ identify.

Proposition 2a

*The one-dimensional Riemann problem associated with the left hand side of* (8)-(11) *has a unique entropy consistent solution* $(\rho, u)$ *composed of constant states* $(\rho_L, u_L)$, $(\rho_1, u_1)$, $(\rho_R, u_R)$ *separated by shock waves and rarefaction waves, with no vacuum occurrence, provided that the initial data* $(\rho_L, u_L), (\rho_R, u_R)$ *agrees with the following condition:*

$$u_R - u_L < g(\rho_L) + g(\rho_R) \tag{16}$$

*still setting:* $g(\rho) = \int_0^\rho \frac{c(a)}{a} da$.

The first part of the proposition is based on the observation that the subsystem of the two conservative equations (9) and (11) is closed, and that it is a classical result that it has a unique entropy-consistent solution provided that initial data agrees with $u_R - u_L < g(\rho_L) + g(\rho_R)$. In order to get some construction of the whole solution, we need to describe more accurately the form of the source term. We will set below $s(\alpha) = \frac{\alpha_{eq} - \alpha}{\tau_0}$, but the proof given is obviously still valid when focusing on many other source terms .

Proposition 2b

*The maximum principle for the void fraction holds for regular solutions. If we assume that the condition* (16) *holds, the maximum principle holds in the one dimensional Riemann problem.*

## III. Fractional step method - FSM

We compute approximations of the solution of the non-homogeneous system using a FSM:

$$\begin{cases} \dfrac{\partial W}{\partial t} + \dfrac{\partial F(W)}{\partial x} = S(W) \\ W(x,0) = W_0(x) \end{cases}$$

At each step of time $t^n \to t^{n+1}$, $W^n \to W^{n+1} = W(.,\Delta t)$, we solve successively the two problems :

$$(P1)\ \ \frac{\partial W^\circ}{\partial t} + \frac{\partial F(W^\circ)}{\partial x} = 0,\ W^\circ(x,0) = W^n(x)$$
$$(P2)\ \ \frac{\partial W}{\partial t} = S(W),\ W(x,0) = W^\circ(x,\Delta t)$$

The problem (P1) corresponds to the computation of approximations of solutions of (5)-(7) using the following classical scheme:

$$\Delta x((W_i^\circ)^{n+1} - W_i^n) + \Delta t(F_{(i,i+1)} - F_{(i-1,i)}) = 0$$

Where $F_{(i,i+1)} = F_{num}(W_i^n, W_{i+1}^n)$ is a two-point numerical flux. The scheme accounts for source terms through (P2).

## IV. Approximate Godunov scheme

### A. Interface solver

We still note: $g(\rho) = \int_0^\rho \frac{c(a)}{a} da$ , with $c(a) = (P'(a))^{1/2}$, and also: $\phi'(\alpha) = -\frac{1}{s(\alpha)}$. The left hand side of system (12)-(15) may be rewritten in terms of the non conservative variable $Y(W) = {}^t(A, \phi, \rho, u)$ in the form:

$$\frac{\partial Y}{\partial t} + C(Y)\frac{\partial Y}{\partial x} = 0 \tag{17}$$

noting:

$$C(Y) = \begin{pmatrix} 0 & 0 & 0 & 0 \\ 1 & u & 0 & 0 \\ 0 & 0 & u & \rho \\ 0 & 0 & \frac{c^2}{\rho} & u \end{pmatrix}$$

We turn now to the associated linearized problem:

$$\frac{\partial Y}{\partial t} + C(\hat{Y}_{LR})\frac{\partial Y}{\partial x} = 0 \tag{18}$$

When noting: $\hat{\lambda}_1 = 0$, $\hat{\lambda}_2 = \hat{u}$, $\hat{\lambda}_3 = \hat{u} - \hat{c}$, $\hat{\lambda}_4 = \hat{u} + \hat{c}$ the right eigenvectors $(\hat{r})_k$ associated with $(\hat{\lambda})_k$ respectively are:

$$\hat{r}_1 = (\hat{u}, -1, 0, 0) \tag{19}$$
$$\hat{r}_2 = (0, 1, 0, 0) \tag{20}$$
$$\hat{r}_3 = (0, 0, \hat{\rho}, -\hat{c}) \tag{21}$$
$$\hat{r}_4 = (0, 0, \hat{\rho}, \hat{c}) \tag{22}$$

and the inverse of the matrix of the right eigenvectors is $(2\rho cu)^{-1}\omega$, where $\omega$ stands for:

$$\begin{pmatrix} 2\rho c & 0 & 0 & 0 \\ 2\rho c & 2\rho cu & 0 & 0 \\ 0 & 0 & uc & -\rho u \\ 0 & 0 & uc & \rho u \end{pmatrix}$$

We note for any quantity $\phi$: $(\Delta\phi)_{LR} = \phi_R - \phi_L$ and $(\overline{\phi})_{LR} = (\phi_R + \phi_L)/2$. Moreover for any $k = 1..4$, $F_{k,l}$ (resp. $F_{k,r}$) denotes the value of $F$ on the left (resp. right) side of the LD field associated with the eigenvalue

$\hat{\lambda}_k$. The computation of the intermediate states in the linearized solver at each interface between two cells labeled $L, R$ is very easy (see[6]). We set here: $\hat{Y} = \overline{Y}$ . Intermediate states for $(A, \phi, \rho, u)$ components are given through (see figure (1)):

$$\rho_1 = \overline{\rho}_{LR} - \frac{\hat{\rho}}{\hat{c}} \frac{(\Delta u)_{LR}}{2} \quad \text{and} \quad u_1 = \overline{u}_{LR} - \frac{\hat{c}}{\hat{\rho}} \frac{(\Delta \rho)_{LR}}{2}$$

The interface solver provides intermediate states of the void fraction which are defined as follows.
If $\hat{u} > 0$, left and right states of $\phi$ on each side of the contact discontinuity $\frac{x}{t} = \lambda_1 = 0$ are:

$$\phi_{1,l} = \phi_L \quad \text{and} \quad \phi_{1,r} = \phi_L - \frac{h}{\hat{u}}$$

If $\hat{u} < 0$, left and right states of $\phi$ on each side of the contact discontinuity $\frac{x}{t} = \lambda_1 = 0$ are:

$$\phi_{1,l} = \phi_R + \frac{h}{\hat{u}} \quad \text{and} \quad \phi_{1,r} = \phi_R$$

Obviously , $A(\frac{x}{t} < 0) = A_L$ and $A(\frac{x}{t} > 0) = A_R$. The figure 1 shows the different states for the case $\hat{u} > 0$, with $\alpha^+ = \alpha(\phi_{1,r})$ and $\alpha^- = \alpha(\phi_{1,l})$. If we restrict to the specific choice $s(\alpha) = \frac{\alpha_{eq} - \alpha}{\tau_0}$, the previous interface solver computes intermediate states which are such that the maximum principle holds for the void fraction $\alpha$.

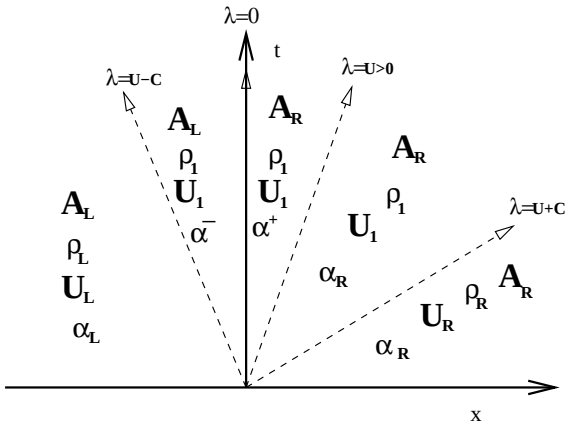


**Figure 1. Summary of solution for $\lambda_2 > 0$.**

## B. Cell schemes

### 1. *First cell scheme*

The application of the approximate Godunov scheme VFRoencv to (8)-(11) yields:

$$A_i^{n+1} - A_i^n = 0 \tag{23}$$

$$\rho_i^{n+1} - \rho_i^n + \frac{\Delta t}{\Delta x} \left( (\rho u)^{*-}_{i+1/2} - (\rho u)^{*+}_{i-1/2} \right) = 0 \tag{24}$$

$$(\rho\alpha)_i^{n+1} - (\rho\alpha)_i^n + \frac{\Delta t}{\Delta x} \left( (\rho\alpha u)^{*-}_{i+1/2} - (\rho\alpha u)^{*+}_{i-1/2} \right) = 0 \tag{25}$$

$$(\rho u)_i^{n+1} - (\rho u)_i^n + \frac{\Delta t}{\Delta x} \left( (\rho u^2 + P(\rho))^{*-}_{i+1/2} - (\rho u^2 + P(\rho))^{*+}_{i-1/2} \right) = 0 \tag{26}$$

The source term $s(\alpha)$ is implicitly contained in the star values, which are given by the interface solver of the preceding section. Thanks to our interface solver, $u$ and $\rho$ are continuous at $\frac{x}{t} = 0$, when using the basic interface solver described above. Both ((24)) and ((26)) are in conservative form.

*2. Second scheme*

The governing equation for the void fraction $\alpha$ is replaced by:

$$\frac{\partial \rho I}{\partial t} + \frac{\partial \rho u I}{\partial x} + \phi \frac{\partial P}{\partial x} = 0 \tag{27}$$

It is easy to verify that this equation is valid for regular solutions. One may also check that jump relations are fulfilled. The equation (27) is discretized, and thus (25) is replaced by:

$$(\rho I)_i^{n+1} - (\rho I)_i^n + \frac{\Delta t}{\Delta x}\left((\rho u)^{*-}_{i+1/2} I^{*-}_{i+1/2} - (\rho u)^{*+}_{i-1/2} I^{*+}_{i-1/2}\right) + \frac{\Delta t}{\Delta x}\hat{\phi}_i^n (P^{*-}_{i+1/2} - P^{*+}_{i-1/2}) = 0 \tag{28}$$

With our interface Riemann solver, we still have $u^{*-}_{i\pm 1/2} = u^{*+}_{i\pm 1/2} = u^*_{i\pm 1/2}$ and $\rho^{*-}_{i\pm 1/2} = \rho^{*+}_{i\pm 1/2} = \rho^*_{i\pm 1/2}$. For all $i$ we replace $I^{*-}_{i+1/2} = A_i + u^*_{i+1/2}\phi^{*-}_{i+1/2}$ and $I^{*+}_{i+1/2} = A_{i+1} + u^*_{i+1/2}\phi^{*+}_{i+1/2}$, where $\phi^{*\pm}_{i+1/2}$ is directly computed by the interface solver, using $Y(W) = {}^t(A, \phi, \rho, u)$ . The equation (28) becomes:

$$(\rho I)_i^{n+1} - (\rho I)_i^n + \frac{\Delta t}{\Delta x}\left((\rho u)^*_{i+1/2} I^{*-}_{i+1/2}) - (\rho u)^*_{i-1/2} I^{*+}_{i-1/2}\right) + \frac{\Delta t}{\Delta x}\hat{\phi}_i^n (P^*_{i+1/2} - P^*_{i-1/2}) = 0 \tag{29}$$

where $\hat{\phi}_i^n = \frac{1}{2}\left(\Phi^{*-}_{i+1/2} + \Phi^{*+}_{i-1/2}\right)$. The next time step requires the computation of $\phi_i^{n+1}$.

$$(\rho u)_i^{n+1}\phi_i^{n+1} = (\rho I)_i^{n+1} - \rho_i^{n+1} A_i \tag{30}$$

## V. Numerical results

All computations performed in this section are based on the use of the previous two cell schemes combined with the above mentionned interface solver (setting $Y(W) = {}^t(A, \phi(\alpha), \rho, u)$). We now provide some results obtained using the FSM and the latter two upwinding schemes. The three test cases have exact unsteady solutions including discontinuities. In the following , the fractional step method, the scheme with standard upwinding of source terms, and the modified scheme including upwinding of source terms are nicknamed $S_{FS}$, $S_{UPW1}$ and $S_{UPW2}$ respectively. The time scale is $\tau_0 = 10^{-4}$ .

### A. Numerical tests

*1. Pure contact discontinuity including a jump of the void fraction $\alpha$*

The initial condition of the Riemann problem will be the following: $\rho_L = \rho_R = 1.$, $U_L = U_R = 10.$, $\alpha_L = 1.$, $\alpha_R = 0.6$. This results in an unsteady contact discontinuity which moves to the right at speed $\sigma = 10$. Both the pressure and the velocity remain uniform over time and space. The exact solution for the void fraction is:

$$\begin{cases} \alpha(x,t) = \alpha_l(t), \ if \ x < \sigma t \\ \alpha(x,t) = \alpha_r(t), \ if \ x > \sigma t \end{cases}$$

The function $\alpha_l(t)$ (resp. $\alpha_r(t)$) is solution of the ODE: $\dfrac{\partial \alpha}{\partial t} = s(\alpha)$, with initial condition $\alpha(0) = \alpha_L$ (resp. with initial condition $\alpha(0) = \alpha_R$ ). Of course, both relax to $\alpha_{eq}$. Owing to the specific choice of the initial condition for the density, the density remains constant. The CFL number is set to 0.5. The solution is plotted at time $Tmax = 3.8\ 10^{-4}$. Both the discrete values of velocity and pressure remain constant (thus

the error is null). A glance at figure (2) clearly shows that the approximate values of the void fraction which have been computed with schemes $S_{FS}$ and $S_{UPW2}$ are almost the same (the error is plot on figure (11)). The scheme $S_{UPW1}$ correctly predicts the position of the contact wave, but amplitudes of $\alpha$ on both sides are not very accurate on a mesh containing 5000 cells.

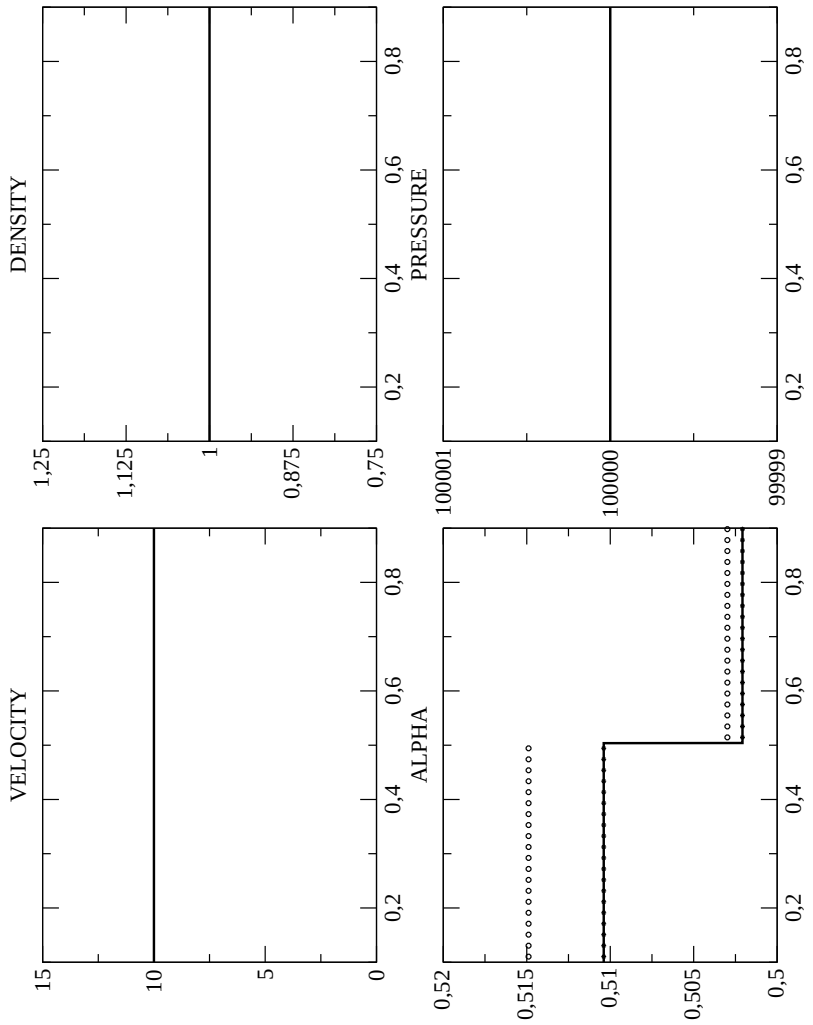


**Figure 2. "Exact" Solution for void fraction discontinuity (5000 cells)**

*2. A standard shock tube with uniform void fraction over space*

We now use the initial condition $U_R = U_L = 10$,$\alpha_L = \alpha_R = 1$, $\rho_L = 1$ and $\rho_R = 0.5$. The CFL number is still equal to 0.5. The solution is plotted at time $Tmax = 3.8\ 10^{-4}$. The scheme $S_{UPW1}$ again provides a rather poor approximation of the solution $\alpha$, but the error is greater, which can easily explained as follows. The local parameter which governs the accuracy on void fraction that is: $1 - e^{-\Delta x/(U_i^n \tau_0)}$, should be an decent approximation of $h/(U_i^n \tau_0)$. It thus clearly appears that in the low Mach number regions, the approximation gets worse, and this is obviously depicted in figure (3). On the other hand, the scheme $S_{FS}$ behaves very

well, but one should keep in mind that this is probably the best set of initial conditions for the latter scheme. The corrected scheme $S_{UPW2}$ performs much better as confirmed by the error analysis below.

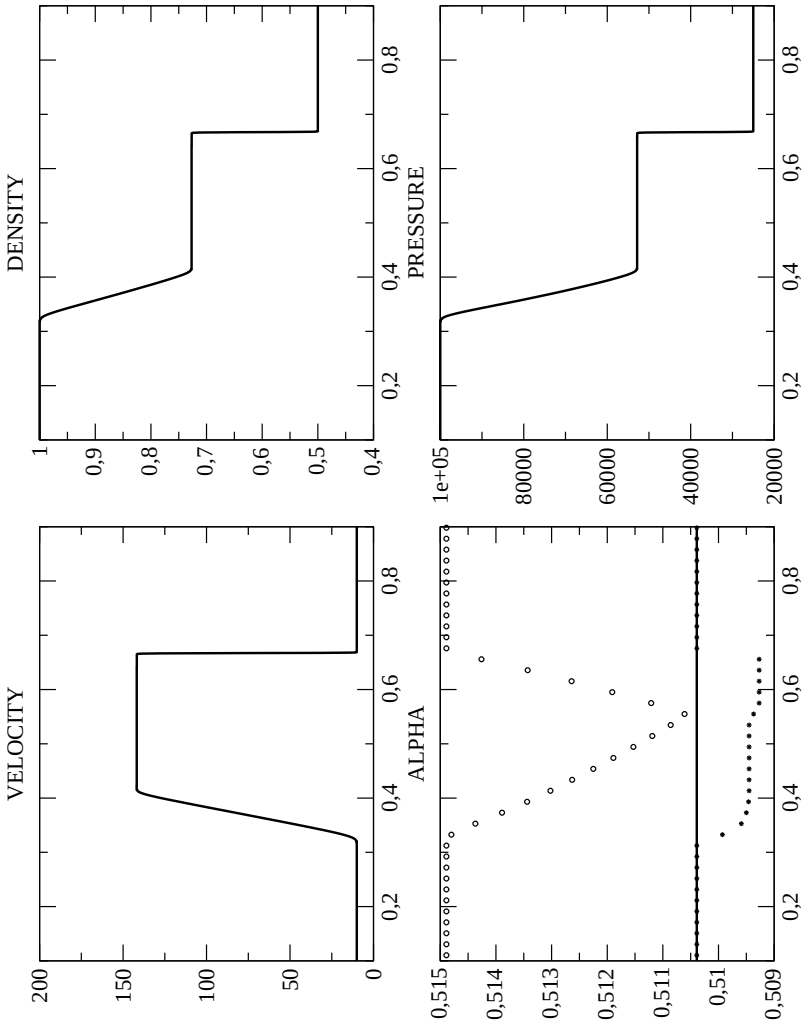


**Figure 3. "Exact" Solution for density discontinuity (5000 cells)**

*3. A standard shock tube with discontinuous initial values of $\alpha$*

The IC now is: $U_R = U_L = 10$, $\alpha_L = 1$ and $\alpha_R = 0.6$ , $\rho_L = 1$ and $\rho_R = 0.5$. The basic solution on $(U, P)$ is the same as in the previous case. Once again, the void fraction steady state is "relaxed" to $\alpha_{eq}$ by the source term, with a two-state pattern as in the first case (there is no influence of the GNL fields on the void fraction profile). The only difference with the first test case is that the speed of the contact discontinuity is now $u = U_l = U_r$ where the $l, r$ subscripts refer to both sides of the contact discontinuity. Hence, the void fraction discontinuity of $\alpha$ moves at speed $u \sim 150$ . Comments pertaining to the three schemes remain almost the same here (see figure (4)). The modified scheme $S_{UPW2}$ performs better in the low Mach number regions, unlike the basic upwinding technique $S_{UPW1}$. The scheme $S_{FS}$ behaves rather well too.

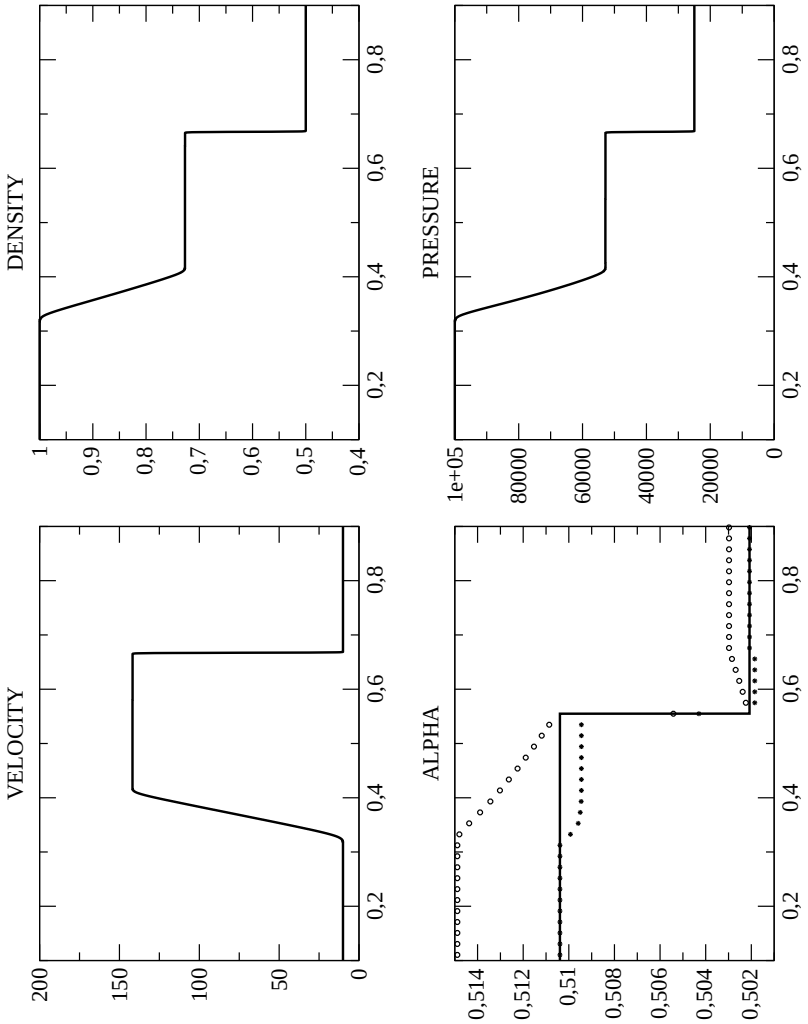


**Figure 4. "Exact" Solution for standard shock tube with discontinuous initial values of $\alpha$**

## B. Physical time scale $\tau_0 = 1e^{-4}$

We still use bold continuous line in order to represent the exact solution, circles to represent the discrete solution for the first cell scheme $S_{UPW1}$, while the stars refer to results obtained with the second cell scheme $S_{UPW2}$. We now plot results obtained with a coarse mesh with 100 cells for: case (A.1) (see figures (5), (6)); case (A.2) (see figures (7), (8)); case (A.3) (see figures (9), (10)). Convergence results for the three cases, and the three schemes, are estimated with a $L_1$ norm. The coarse mesh contains 100 cells and the finest one 150000. Here again, circles denote results obtained with $S_{UPW1}$ scheme while stars are used for $S_{UPW2}$ scheme, but here the bold line stands for $S_{FS}$ scheme. The first graphic in figure (11) represents the first Rieman problem (section V.A.1), the second figure the second Rieman problem (section V.A.2), and the third one the third Rieman problem (section V.A.3). Similar results for $\tau_0 = 1e^{-3}$ and $\tau_0 = 1e^{-6}$ can be found in.[17]

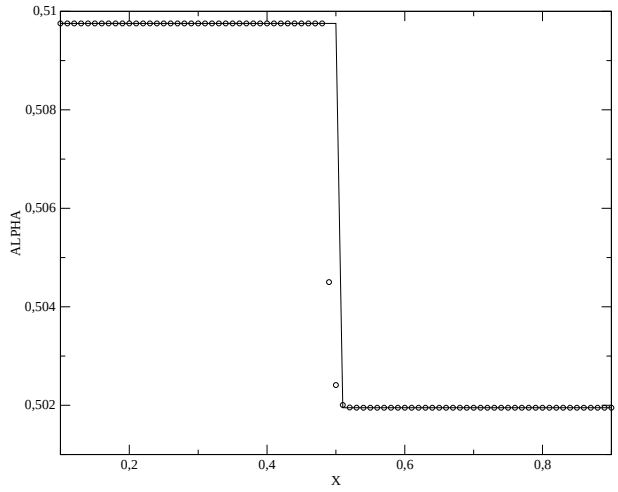


**Figure 5. Fractional step method - 100 cells -**

## VI. Conclusion

The two shemes $S_{UPW2}$ and $S_{FS}$ have a similar behavior. The first one $S_{UPW2}$ is the best one for steady computations, the second one is favoured when highly time dependent solutions develop, especially if convective terms are negligible when compared with (stiff) source terms. If $\Delta t \ll \tau_0$, $S_{FS}$ performs quite well. Moreover, the scheme $S_{UPW1}$ is excellent for *steady* computations ; nonetheless, if $\frac{\Delta x}{U_0 \tau_0}$ is not small compared with 1, the scheme $S_{UPW1}$ provides rather poor (though convergent) results in highly *unsteady* cases. This is obviously not in favour of low Mach number areas or small time scales.

## Acknowledgments

This work has received financial support from the NEPTUNE project.

## References

[1]L. Gosse , A well balanced flux splitting scheme designed for hyperbolic systems of conservation laws with source terms , *Computers and Mathematics with Applications*, 2000, vol. 39, pp. 135–159.

[2]L. Gosse , A well balanced flux splitting scheme using non conservative products designed for hyperbolic systems of conservation laws with source terms , *Math. Mod and Meth. in Appl. Sciences*, 2001, vol. 70, pp. 339–365.

[3]L. Gosse and A.Y. LeRoux, Un schéma équilibre adapté aux lois de conservation scalaires non homogènes, *Comptes Rendus Académie des Sciences de Paris*, 1996, vol. I-323, pp. 543–546.

[4]J.M. Greenberg and A.Y. LeRoux, A well balanced scheme for the numerical processing of source terms in hyperbolic equations, *SIAM J. of Num. Anal.*, 1996, vol. 33, pp. 1–16.

[5]A.Y. LeRoux, Discrétisation de termes sources raides dans les problèmes hyperboliques, *Cours CEA-EDF-INRIA*, 1998, INRIA Rocquencourt, France.

[6]T. Buffard, T. Gallouët and J.M. Hérard, A sequel to a rough Godunov scheme. Application to real gases, *Computers and Fluids*, 2000, vol. 29-7, pp. 813–847.

[7]T. Gallouët, J.M. Hérard and N. Seguin, Some recent Finite Volume schemes to compute Euler equations using real gas EOS, *Int. J. for Num. Meth. in Fluids*, 2002, vol. 39(12), pp. 1073-1138.

[8]T. Gallouët, J.M. Hérard and N. Seguin, Some approximate Godunov schemes to compute shallow water equations with topography, *Computers and Fluids*, 2003, vol. 32(4), pp.479-513.

[9]E. Godlewski and P.A. Raviart, *Numerical approximation of hyperbolic systems of conservation laws*, Springer Verlag, 1996.

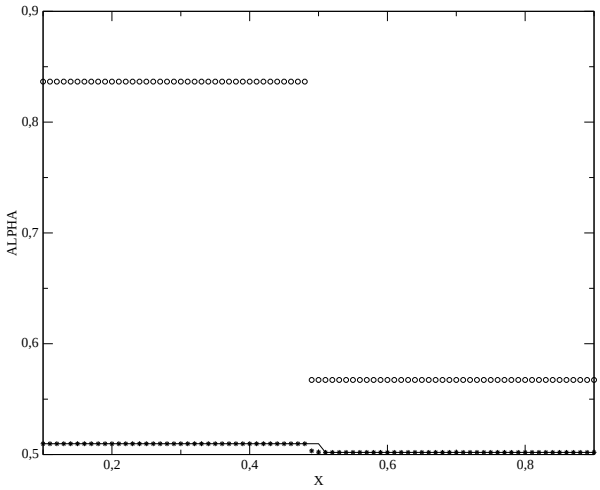


**Figure 6. First and second cell schemes for Leroux method - 100 cells -**

[10]S.K. Godunov, A difference method for numerical calculation of discontinuous equations of hydrodynamics, *Mat. Sb.*, 1959, pp. 271–300. In Russian.

[11]A. Guelfi et al, A new multiscale platform for advanced nuclear thermal hydraulics: status and perspectives of the NEPTUNE project, *to appear in the proceedings of NURETH 11*, 2005.

[12]A. Ambroso, An introduction to the problem of interfacial coupling of thermohydraulic models, *CEA report SFME/LETR/04/008/A*, 2004.

[13]A. Ambroso, C. Chalons, F. Coquel, E. Godlewski, F. Lagoutiere, P.A. Raviart, N. Seguin and J.M. Herard, Coupling of multiphase flow models, *to appear in the proceedings of NURETH 11*, 2005.

[14]J.M. Herard, Naive schemes to couple isentropic flows between free and porous medium, *internal EDF report HI-81/04/08/A*, 2004.

[15]J.M. Herard and O. Hurisse, Coupling two and one dimensional model through a thin interface, *AIAA paper 2005-4718*.

[16]J.M. Herard and O. Hurisse, On the coupling of HEM and HRM models through a thin interface, *in preparation*.

[17]J.M. Herard and O. Hurisse, A few schemes to compute hyperbolic systems with source terms, *EDF report HI-81/04/07/A*, 2004.

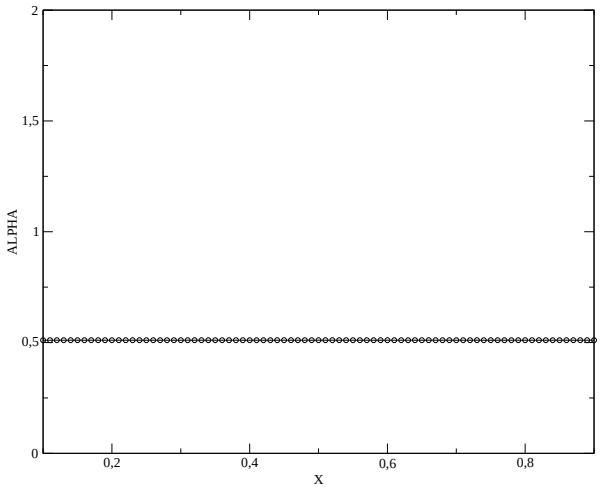


**Figure 7. Fractional step method - 100 cells -**

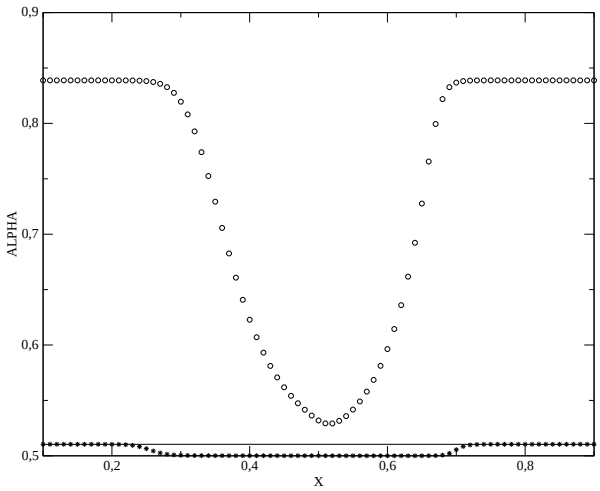


**Figure 8. First and second cell schemes for Leroux method - 100 cells -**

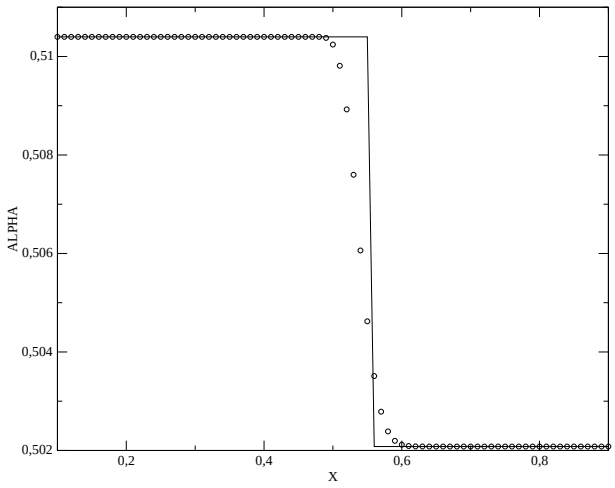


**Figure 9. Fractional step method - 100 cells -**

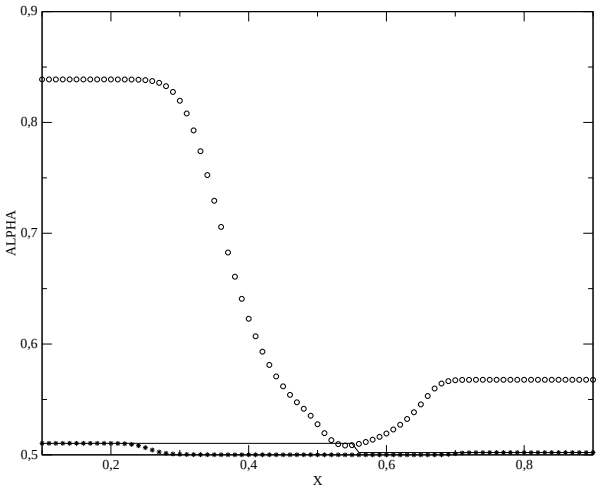


**Figure 10. First and second cell schemes for Leroux method - 100 cells -**

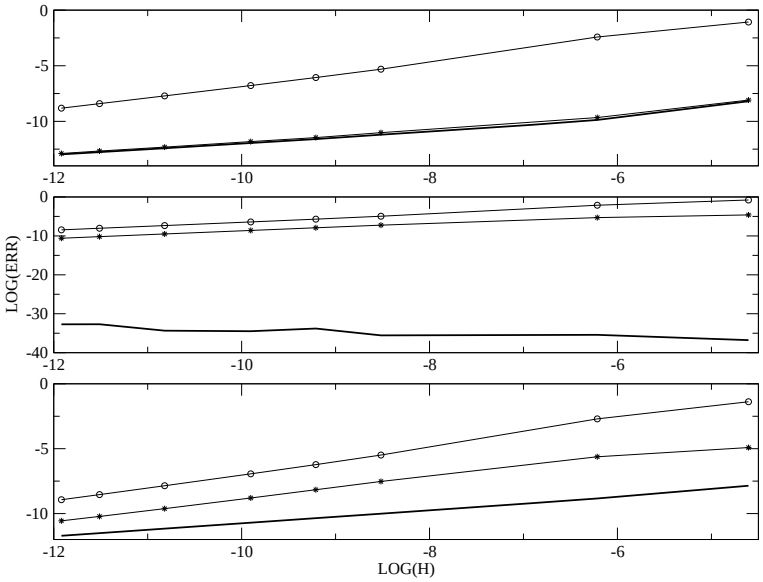


**Figure 11. Convergence in $L_1$ norm**